

# Wireless Power Transfer for Electric Vehicles Application using the Principle of ICPT System

Jigyasa Chand

Eight Semester UG Scholar  
Department of Electrical and  
Electronics Engineering,  
Dr.T.Thimmaiah Institute of  
Technology, Kolar Gold Fields-  
563120,Karnataka, India.  
jigyasac.kvgonda@gmail.com

Anjali. P.S

Eight Semester UG Scholar  
Department of Electrical and  
Electronics Engineering,  
Dr.T.Thimmaiah Institute of  
Technology, Kolar Gold Fields-  
563120,Karnataka, India  
psanjali1997@gmail.com

Kirthiga G

Eight Semester UG Scholar  
Department of Electrical and  
Electronics Engineering,  
Dr.T.Thimmaiah Institute of  
Technology, Kolar Gold Fields-  
563120,Karnataka, India.  
kirthigaganeshan02658@gmail.com

B. Somashekar

Assistant professor,  
Department of Electrical and Electronics Engineering,  
Dr.T.Thimmaiah Institute of Technology,  
Kolar Gold Fields-563120,Karnataka, India.  
soma0103@yahoo.co.in,somashekar@drtit.edu.in

**Abstract:** Wireless Power Transfer is method of transferring the power from the power source to the electrical load without the physical contact, by using the principle of magnetic resonance. Due to the increase in the cost of the petroleum product and environmental issues led to development of the Electrical Vehicles (EV's) globally for transportation. The charging of electric vehicles using wire causes losses therefore, it decrease in efficiency of the system. The preliminary review of the WPT analysis tells that the Inductively Coupled Power Transfer system ICPT is one of the promising and convenient methods for charging the EV's. The paper is about designing the circuit using the MATLAB Simulink Software .The results for different values of load versus Efficiency of the system of ideal case is been plotted were the maximum efficiency is around 98% assuming the alignment errors as zero. The system parameters and performance equations are coded using MATLAB for Model based design for charging the EV application. Also, efficiency and load curve characteristics are demonstrated. The paper demonstrates the experimental setup of the same for the distance of about 15 cm. Each part of the setup and the components used along with their features has been discussed briefly. The same setup for higher power rating can be implemented in future with design modifications.

**Keywords** — *Wireless Power Transfer (WPT), MATLAB Simulation,Inductively Coupled Power Transfer system ( ICPT), Pulse Width Modulator (PWM) Generators.*

\*\*\*\*\*

## I. INTRODUCTION

All conventional vehicles are powered by an internal combustion engine (ICE) only. These conventional vehicle produce exhaust gases during operation which are harmful for human health. But electric vehicles (EVs) run on electricity only. They are propelled by one or more electric motors which are powered by rechargeable battery packs. Due to this electric vehicles have several advantages over conventional vehicles. No harmful gas emission. Fuel cost will be up to 70% less than conventional vehicle, maintenance cost is less, ideal for stop-start city driving as

No energy is utilise when the vehicle is stationary.[6][7]

Besides the high initial cost, the long charging time of EV batteries also makes the EV not acceptable to many drivers. For a single charge, it takes about one half-hour to several hours depending on the power level of the charger, which is

many times longer than the gasoline refuelling process. The EVs cannot get ready immediately when they have run out of battery. Because of this, the owner has to find any possible opportunity to plug-in and charge the battery. It really brings trouble as people may forget to plug-in and find themselves out of battery energy later on. The charging cables on the floor may lead to tripping hazards. Leakage from cracked old cable, particularly in cold zones, can bring additional hazardous conditions to the owner. Also, people May have to brave the wind, rain, ice, or snow to plug-in with the risk of getting an electric shock. The wireless power transfer (WPT) technology, which can eliminate all the charging trouble, is therefore most desirable by the EV owners. By wirelessly transferring energy to the EV, the charging becomes the easiest task. For a stationary WPT system, the drivers just have to park their car and leave. Also

the battery capacity of EVs with wireless charging could be reduced to 20% or less compared to EVs with conductive charging.

## II.BLOCK DIAGRAM

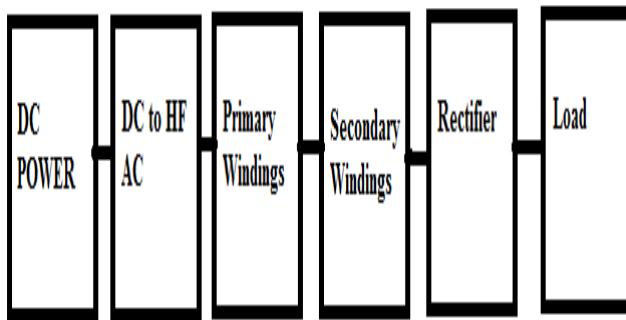


**Fig.1 Block diagram of EV's**

The power source is of DC supply that supplies the electricity to the load of the EV. The dc supply of 150V is supplied to the; electric Vehicle.

The inverter circuit is used to convert the DC to high frequency AC. The inverter will contain the four MOSFETs where two MOSFETs are driven at a time with the help of power generators and further it is connected to primary coil and the power is transferred from primary to secondary coil through the principle of resonant circuit. By resonating with the secondary windings compensation network the power is transferred, then the AC current is rectified using the power electronics converters and charged to the batteries.

## III.ICPT SYSTEM

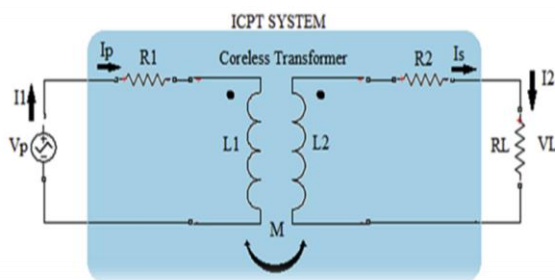


**Fig.2 Equivalent circuit of electric vehicles**

Uncompensated circuit model of inductive magnetic coupled power transfer system, which makes understanding the system easy is seen in Fig. 1. This is the most fundamental figure. Here,  $V_1$  is rms value of sinusoidal signal applied to primary winding. Assuming that voltage and current are sinusoidal, the induced voltage in secondary winding due to the primary current  $I_p$  is  $j\omega MI_p$ , reflected voltage in the primary winding due to the secondary current  $I_s$  is  $j\omega MI_s$  where "M" is the mutual inductance and  $\omega$  is the operation frequency. Mathematical equation of system's equivalent circuit must be derived in order to follow power flow of ICPT system. According to equivalent circuit, Eq. (1) can be written for input Voltage  $V_p$

$$V_p = [R_p + j(\omega L_p)]I_p - j\omega MI_s \text{-----[1]}$$

$$V_p = [R_p + j(X_p)]I_p - j\omega MI_s$$

$$V_p = [Z_p]I_p - j\omega MI_s$$

ICPT systems provide high efficiency at low power, low frequency such as 50-60 Hz and at high mutual inductance. However, when high power is concerned, power transmission becomes more difficult. System must have an appropriate magnetic coupling coefficient at high resonance frequency. Furthermore, it is realized that losses which may occur in the system affect the efficiency of the system. For this reason, these systems are operated at resonance frequency in order to minimize the losses. Despite this, the operating frequency is usually under 100 kHz for high power applications due to switching losses [21].

Besides, Litz wire is used to reduce skin effect and proximity effect losses which occur in windings [8, 11] magnetic coupling coefficient (k) is a value which shows how much of the magnetic flux created by the primary is transferred to the secondary circuit. Therefore, the efficiency of the power transferred from the primary to the secondary depends on the magnetic coupling coefficient. The magnetic coupling coefficient is given in Eq. (2).

$$K = \frac{M}{\sqrt{L_p L_s}} \text{-----[2]}$$

It can be seen that the mutual inductance and the magnetic coupling coefficient have a strong impact on each other. But, it does not mean that an increase in mutual inductance increases the magnetic coupling coefficient. Other determining parameters are the primary and the secondary inductance values. According to this, it is understood that the windings must have optimal parameter values.

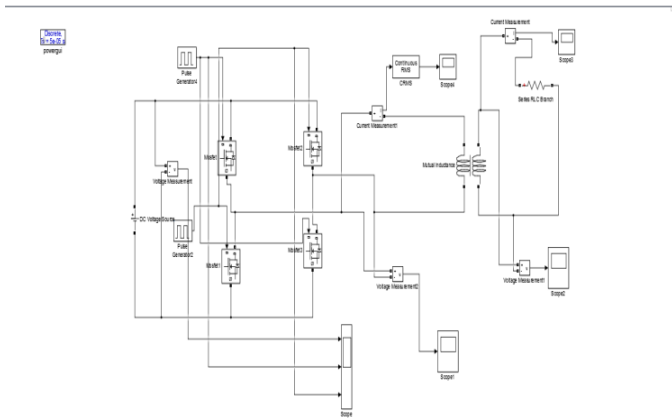
The magnetic coupling coefficient must be within a certain range depending on the compensation topology. There must be a strong magnetic connection between the primary and secondary windings in order to provide high efficient power transfer. Increase in air gap between the windings decreases the magnetic coupling coefficient and systems which have magnetic coupling coefficient under 0.2 are accepted as low magnetic coupled systems.

In addition, the air gap distances between the windings must be homogenous and the winding conductors must be aligned. In the absence of this alignment the magnetic connection will not be strong and this reduces the system efficiency. In air-gapped transformers, the coupling coefficient and the quality factors (Q) of the windings are two important parameters. The quality factor reflects a large magnetic field and minimal loss creation capacity of the windings.

The relationship between the secondary reactive and active power has been given in Eq. (3) which is considered to be equal to the secondary winding quality factor [11].

$$Q_s = \frac{\omega_0 L_s}{R_l} \text{-----[3]}$$

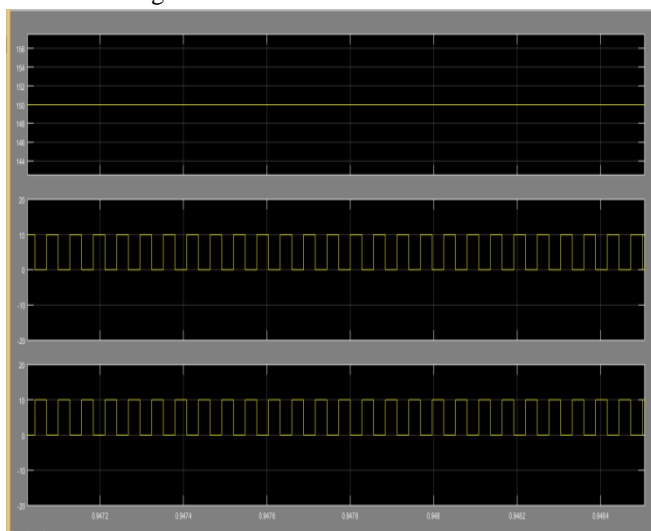
#### IV.Simulated Circuit Using MATLAB



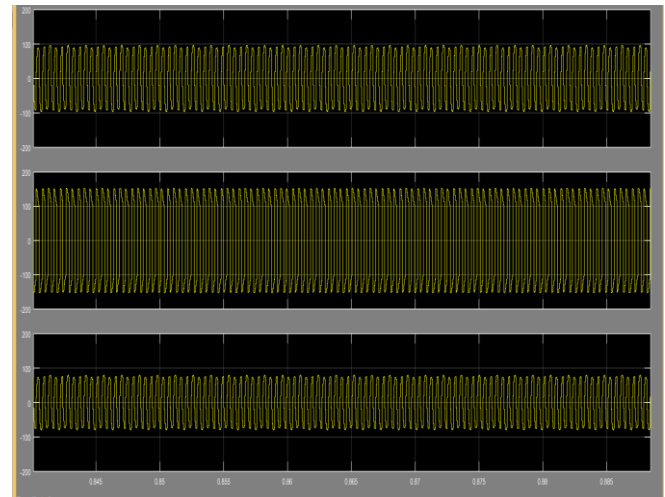
**Fig no.3 Simulated Circuit Using MATLAB**

Fig shows the simulated circuit ,which is developed using the MATLAB simulation ,here the circuit is designs for an ideal case where the misalignment in the circuit is zero between the primary and secondary compensation circuit .The input supply is of 150v DC ,and the mutual inductance of 12,175microH.ICPT System is supplied by the H bridge inverter circuit with the resonating principle, the power is transferred from primary to secondary side to the resistive load of 1.215.The efficiency of the circuit is found to be around 98% .

The input DC of 150v is shown in the fig3.1 and the waveforms of the generator circuit is shown in fig3.2 and 3.3.The fig4.1 shows the AC source after inverting the 150 DC to high frequency ac source across the primary compensation circuit. Fig 4.2 and 4.3 is the output waveforms of current and voltage which is obtained across the load. As the load is increased the efficiencies decreased this was observed and tabulated as shown in the table 1 and the graph if shown in the fig 5.



**Fig no.4Input And Output Graphs Using the MATLAB Simulation Input Waveforms Of Supply And Pulse Generator 1 And 2**



**Fig.5.Output wave forms of voltmeters which is connected to primary winding side and secondary winding and output current waveforms**

#### V. Results of Simulated circuit

Load resistance in ohms	Efficiency of the simulated circuit
2	98.96
4	98.59
6	98.08
8	97.54
10	96.99
12	96.44
14	95.60

**Table.I .Load resistance verses Efficiency**

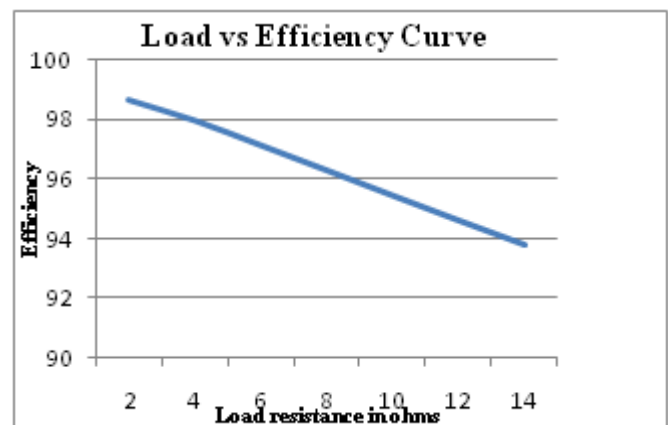
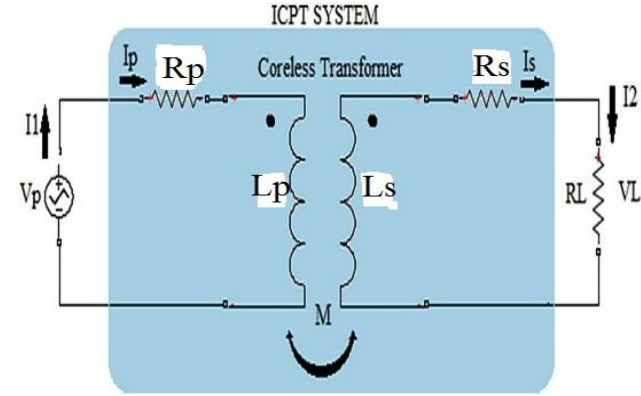


**Fig no.6 load versus efficiency**

#### VI.INDUCTIVELY COUPLED WIRELESS POWER TRANSFER SYSTEM

The inductively coupled power transfer (ICPT) method is known worldwide for its high power transfer in many applications, mainly in electric vehicles [5,7]. It provides a

rapid charging process, and optimized power transmission by frequency variation and control over the loss due to low magnetic coupling. The ICPT has been used for both stationary and moving electric vehicles [4]. If the vehicle being charged is stationary, it is said to be “charging of the battery electric vehicle (BEV)” or “static charging”,



### DESIGN OF ICPT CIRCUIT PARAMETERS

The primary and secondary windings resistance is given as follows

$$R_p = \frac{\rho_{cu} * N_p * 2(a_1 + b_1)}{S_p}$$

$$R_s = \frac{\rho_{cu} * N_s * 2(a_2 + b_2)}{S_s}$$

Here Litz wire is used for winding as it negligible proximity error and skin effect

$\rho_{cu}$  = Resistivity of wire.

The primary and secondary inductance is given by

$$L_p = \frac{\mu_0 N_p^2 \left[ a_1 \ln \frac{2a_1 b_1}{r_1(a_1 + \sqrt{a_1^2 + b_1^2})} + b_1 \ln \frac{2a_1 b_1}{r_1(b_1 + \sqrt{a_1^2 + b_1^2})} - 2(a_1 + b_1 - \sqrt{a_1^2 + b_1^2}) + .25(a_1 + b_1) \right]}{\pi}$$

$$L_s = \frac{\mu_0 N_s^2 \left[ a_2 \ln \frac{2a_2 b_2}{r_2(a_2 + \sqrt{a_2^2 + b_2^2})} + b_2 \ln \frac{2a_2 b_2}{r_2(b_2 + \sqrt{a_2^2 + b_2^2})} - 2(a_2 + b_2 - \sqrt{a_2^2 + b_2^2}) + .25(a_2 + b_2) \right]}{\pi}$$

Mutual inductance is given by

$$M = \frac{\mu_0 N_s N_p}{\pi} \left[ a_1 \ln \frac{(a_1 + (\sqrt{h^2 + a_1^2}) + (\sqrt{h^2 + b_1^2}))}{(a_1 + \sqrt{h^2 + a_1^2 + b_1^2})h} + b_1 \ln \frac{(b_1 + (\sqrt{h^2 + a_1^2}) + (\sqrt{h^2 + b_1^2}))}{(b_1 + \sqrt{h^2 + a_1^2 + b_1^2})h} - 2(h - (\sqrt{h^2 + a_1^2}) + (\sqrt{h^2 + b_1^2})) + \sqrt{h^2 + a_1^2 + b_1^2} \right]$$

Coupling Co-efficient (k)

The power transfer capability of an ICPT system depends on the coupling coefficient [1] which is given by

$$K = \frac{M}{\sqrt{L_p L_s}}$$

System frequency is

$$\omega_0 = \frac{1}{\sqrt{L_s C_s}} = \frac{1}{\sqrt{L_p C_p}}$$

The primary and secondary impedances

$$Z_p = R_p + j \left( \omega L_p - \frac{1}{\omega C_p} \right) + \frac{C_s M^2 \omega^3}{\omega C_s (R_s + R_l) + j(\omega^3 L_s C_s - 1)}$$

$$Z_s = R_s + R_l + j \left( \omega L_s - \frac{1}{\omega C_s} \right)$$

Primary voltage is equal to

$$V_p = [R_p + j(\omega L_p)] I_p - j\omega M I_s$$

$$V_p = [R_p + j(X_p)] I_p - j\omega M I_s$$

$$V_p = [Z_p] I_p - j\omega M I_s$$

Primary current  $I_p$

$$I_p = V_p / Z_p$$

Secondary current

$$I_s = \frac{j\omega M I_p}{Z_s}$$

Secondary winding voltage

$$V_l = j\omega M I_p - \left( R_s + j \left( \omega L_s - \frac{1}{\omega C_s} \right) \right) I_s$$

Secondary impedance referred to primary is given as

$$Z_r = \frac{\omega^2 M^2}{Z_s}$$

Power transferred from primary to secondary side

$$P = \text{Re} \{ Z_r | I_p|^2 \}$$

### VL COIL CONFIGURATION

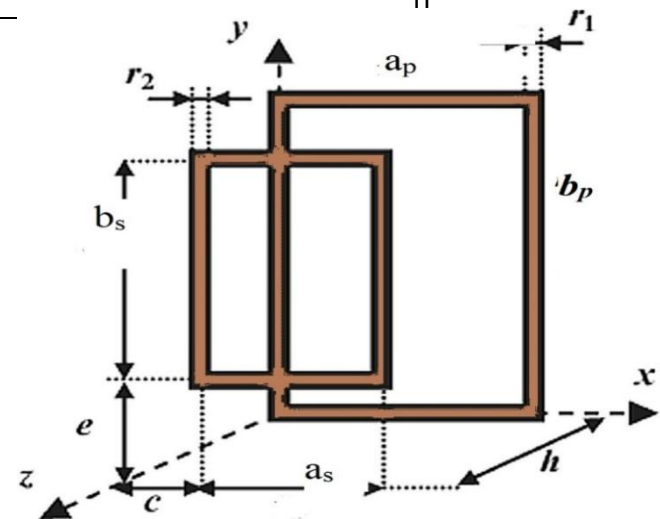


Figure 7: Rectangular geometry winding

The width of primary and secondary windings is denoted as  $a_p$  and  $a_s$  respectively. The length of primary and secondary windings is denoted as  $b_p$  and  $b_s$  respectively.  $N_p$  and  $N_s$  are primary and secondary turns.  $S_p$  and  $S_s$  are surface area of primary and secondary winding. 'h' denotes air gap distance between primary and secondary winding. 'c' and 'e' are alignment error values. Single side length of primary and secondary windings is

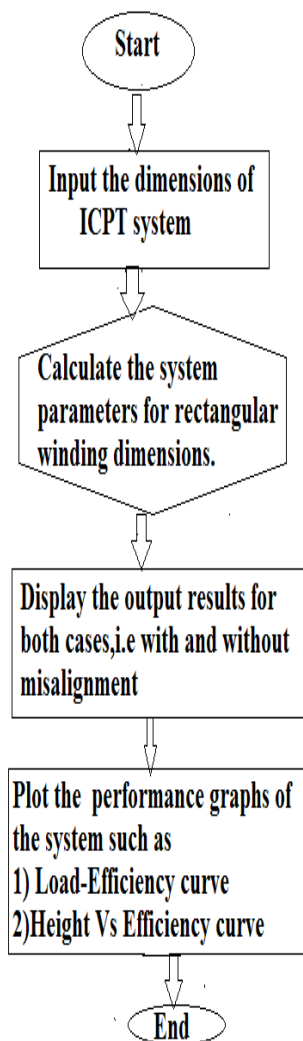
$$r1 = \sqrt{\frac{N_p S_p}{\pi}}$$

$$r2 = \sqrt{\frac{N_s S_s}{\pi}}$$

Efficiency of the system is given as

$$\eta = \frac{R_l}{R_l + R_s} \left( \frac{1}{1 + R_p \frac{(R_l + R_s)}{\omega^2 M^2}} \right)$$

### VIII.FLOW CHART OF MAT LAB PROGRAMMING



Mat lab programming

```

clc;
clear all;
h=input('height in m =');
a1=input('width of primary winding in m =');
a2=input('width of secondary winding in m =');
b1=input('length of primary winding in m =');
b2=input('length of secondary winding in m =');
vp=input(' primary voltage in volts =');
RL=input(' load resistance in ohms =');
Np=input('primary turns =');
Ns=input('secondary turns =');
Sp=input(' primary surface area in mm^2 =');
Ss=input(' secondary surface area in mm^2 =');
pcu=input(' Resistivity of copper =');
f=input('frequency in Hz =');
% setting alignment errors
c=0;
e=0;
% to find single side lengths of pri and sec r1 and r2
r1=sqrt((Np*Sp)/pi);
r2=sqrt((Ns*Ss)/pi);
% to find pri and sec winding resistance
Rp=(pcu*Np*2*(a1+b1))/Sp;
Rs=(pcu*Ns*2*(a2+b2))/Ss;
% to compute Lp&Ls
mu=4*pi*10^(-7);
p=sqrt(a1^2 + b1^2);
q=sqrt(a2^2 + b2^2);
Lp=[mu*Np*Np*(a1*log((2*a1*b1)/(r1*(a1+p)))+b1*log((2*a1*b1)/(r1*(b1+p)))-2*(a1+b1-p)+0.25*(a1+b1))]/pi;
Ls=[mu*Ns*Ns*(a2*log((2*a2*b2)/(r2*(a2+q)))+b2*log((2*a2*b2)/(r2*(b2+q)))-2*(a2+b2-q)+0.25*(a2+b2))]/pi;
% to compute mutual inductance
r=sqrt(h^2+a1^2);
s=sqrt(h^2+b1^2);
t=sqrt(h^2+a1^2+b1^2);
M2=[(mu*Ns*Np)*(a1*log((a1+r*s)/(a1+h*t))+b1*log((b1+r*s)/(b1+h*t)) -2*(h-r-s+t))/pi;
d=a1-a2-c;
m=a2+c;
q=b2+e;
g=a1-c;
p=b1-e;
t=b1-b2-e;
A=sqrt(h^2+t^2+d^2);
B=sqrt(h^2+d^2+q^2);
C=sqrt(h^2+q^2+g^2);
D=sqrt(h^2+g^2+t^2);
E=sqrt(h^2+q^2+c^2);
F=sqrt(h^2+c^2+t^2);
G=sqrt(h^2+t^2+m^2);
H=sqrt(h^2+m^2+q^2);
    
```



```

B1=(d*log((d+A)/(d+B))+h*log((g+C)/(g+D))+c*log((-
c+E)/(-c+F))+m*log((-m+G)/
(-m+H))+ B-C-H+E+D-A+G-F);
I=sqrt(h^2+p^2+d^2);
J=sqrt(h^2+d^2+e^2);
K=sqrt(h^2+e^2+g^2);
L=sqrt(h^2+p^2+h^2);
M=sqrt(h^2+e^2+c^2);
N=sqrt(h^2+c^2+p^2);
O=sqrt(h^2+p^2+m^2);
P=sqrt(h^2+m^2+e^2);
Q=sqrt(h^2+p^2+g^2);
B2=(d*log((d+h)/(d+J))+g*log((h+K)/(g+L))+c*log((-c+M)/(-
c+N))+m*log((-m+O)/(-m+P))+J-K-P+M+Q-I+O-N);
R=sqrt(h^2+g^2+t^2);
S=sqrt(h^2+t^2+c^2);
T=sqrt(h^2+p^2+c^2);
U=sqrt(h^2+g^2+p^2);
V=sqrt(h^2+e^2+c^2);
W=sqrt(h^2+e^2+g^2);
X=sqrt(h^2+g^2+q^2);
Y=sqrt(h^2+c^2+q^2);
B3=(t*log((t+R)/(t+S))+p*log((p+T)/(p+U))+e*log((-e+V)/(-
e+W))+q*log((-q+X)/(-q+Y))+S-T-Y+V+U-R+X-W);
Z=sqrt(h^2+d^2+t^2);
A1=sqrt(h^2+t^2+m^2);
A2=sqrt(h^2+m^2+p^2);
A3=sqrt(h^2+d^2+p^2);
A4=sqrt(h^2+e^2+m^2);
A5=sqrt(h^2+e^2+d^2);
A6=sqrt(h^2+d^2+q^2);
A7=sqrt(h^2+m^2+q^2);
B4=(t*log((t+Z)/(t+A1))+p*log((p+A2)/(p+A3))+e*log((-
e+A4)/(-e+A5))+q*log((-q+A6)/(-q+A7))+      A1-A2-A7-
A4+A3-Z+A6-A5);
M3=(mu*Np*Ns)/(4*pi)*(B1-B2+B3-B4);
%to compute coefficient of coupling
k1= M2 /(sqrt(Lp*Lv));
k2=M3/(sqrt(Lp*Lv));
%to compute capacitance for SS compensation
w= 2*pi*f;
Cp= 1/(w*w*Lp)
Cs= 1/(w*w*Ls)
% to find quality factor
Qp1= (Lp*RL)/(w*M2^2);
Qp2=(Lp*RL)/(w*M3^2);
Qs=(w*Ls)/(RL);
% to compute distribution factor
Kd=(1/((1+log(Qp1/Qs))*(1+log(fm/f))));
% To compute load voltage & power
Zs= Rs +RL +((w*Ls)-(1/(w*Cs)))*i
Zr1 =((w*M2)^2)/Zs
Zr2 =((w*M3)^2)/Zs

```

```

Zp1=Rp+((w*Lp)-(1/(w*Cp)))*i +Zr1
Zp2=Rp+((w*Lp)-(1/(w*Cp)))*i +Zr2
Ip1= vp/Zp1
Ip2=vp/Zp2
Is1=(w*M2*Ip1)/Zs
Is2=(w*M3*Ip2)/Zs
Vl1=real(RL*Is1)
Vl2=real(RL*Is2)
P1=real(Zr1)*Ip1^2;
P2=real(Zr2)*Ip2^2;
eff1=(RL/(RL+Rs))*(1/(1+Rp*(RL+Rs)/(w^2*M2^2)));
eff2=(RL/(RL+Rs))*(1/(1+Rp*(RL+Rs)/(w^2*M3^2)));
fprintf('parameters are as follows');
fprintf('\n the number of primary turns Np=%f',Np);
fprintf('\n the number of secondary turns Ns=%f',Ns);
fprintf('\n the primary surface area Sp=%f',Sp);
fprintf('\n the secondary surface area Ss=%f',Ss);
fprintf('\n the single side length of primary r1=%f',r1);
fprintf('\n the single side ltheength of secondary r2=%f',r2);
fprintf('\n the primary winding resistance Rp=%f',Rp);
fprintf('\n the secondary winnding resistance Rs=%f',Rs);
fprintf('\n the primary winding inductance Lp=%f',Lp);
fprintf('\n the secondary winding inductance Lv=%f',Lv);
fprintf('\n the mutual inductance without misalignment
M2=%f',M2);
fprintf('\n the mutual inductance with misalignment
M3=%f',M3);
fprintf('\n the coefficient of coupling without misalignment
k1=%f',k1);
fprintf('\n the coefficient of coupling with misalignment
k2=%f',k2);
fprintf('\n the frequency of the system f=%f',f);
fprintf('\n the capacitance of the primary system C1=%f',Cp);
fprintf('\n the capacitance of the secondary system
C2=%f',Cs);
fprintf('\n the secondary winding voltage without
misalignment Vl1=%f',Vl1);
fprintf('\n the secondary winding voltage with misalignment
Vl2=%f',Vl2);
fprintf('\n the quality factor of primary winding without
misalignment Qp1=%f',Qp1);
fprintf('\n the quality factor of primary winding with
misalignment Qp2=%f',Qp2);
fprintf('\n the quality faactor of secondary winding
Qs=%f',Qs);
fprintf('\n the power transfer from primary to secondary
without misalignment P1=%f',P1);
fprintf('\n the power transfer from primary to secondary with
misalignment P2=%f',P2);
fprintf('\n the efficiency of the system without misalignment
eff1=%f',eff1);
fprintf('\n the efficiency of the system with misalignment
eff2=%f',eff2);

```

### Plot of load resistance vs. distribution factor

```
h=0:0.1:10;  
A=sqrt(h.^2+t.^2+d.^2);  
B=sqrt(h.^2+d.^2+q.^2);  
C=sqrt(h.^2+q.^2+g.^2);  
D=sqrt(h.^2+g.^2+t.^2);  
E=sqrt(h.^2+q.^2+c.^2);  
F=sqrt(h.^2+c.^2+t.^2);  
G=sqrt(h.^2+t.^2+m.^2);  
H=sqrt(h.^2+m.^2+q.^2);  
B1=(d.*log((d+A)./(d+B))+h.*log((g+C)./(g+D))+c.*log((-  
c+E)./(-c+F))+m.*log((-m+G)./(-m+H))+B-C-H+E+D-A+G-  
F);  
I=sqrt(h.^2+p.^2+d.^2);  
J=sqrt(h.^2+d.^2+e.^2);  
K=sqrt(h.^2+e.^2+g.^2);  
L=sqrt(h.^2+p.^2+h.^2);  
M=sqrt(h.^2+e.^2+c.^2);  
N=sqrt(h.^2+c.^2+p.^2);  
O=sqrt(h.^2+p.^2+m.^2);  
P=sqrt(h.^2+m.^2+e.^2);  
Q=sqrt(h.^2+p.^2+g.^2);  
B2=(d.*log((d+h)./(d+J))+g.*log((h+K)./(g+L))+c.*log((-  
c+M)./(-c+N))+m.*log((-m+O)./(-m+P))+J-K-P+M+Q-I+O-  
N);  
R=sqrt(h.^2+g.^2+t.^2);  
S=sqrt(h.^2+t.^2+c.^2);  
T=sqrt(h.^2+p.^2+c.^2);  
U=sqrt(h.^2+g.^2+p.^2);  
V=sqrt(h.^2+e.^2+c.^2);  
W=sqrt(h.^2+e.^2+g.^2);  
X=sqrt(h.^2+g.^2+q.^2);  
Y=sqrt(h.^2+c.^2+q.^2);  
B3=(t.*log((t+R)./(t+S))+p.*log((p+T)./(p+U))+e.*log((-  
e+V)./(-e+W))+q.*log((-q+X)./(-q+Y))+S-T-Y+V+U-R+X-  
W);  
Z=sqrt(h.^2+d.^2+t.^2);  
A1=sqrt(h.^2+t.^2+m.^2);  
A2=sqrt(h.^2+m.^2+p.^2);  
A3=sqrt(h.^2+d.^2+p.^2);  
A4=sqrt(h.^2+e.^2+m.^2);  
A5=sqrt(h.^2+e.^2+d.^2);  
A6=sqrt(h.^2+d.^2+q.^2);  
A7=sqrt(h.^2+m.^2+q.^2);  
B4=(t.*log((t+Z)./(t+A1))+p.*log((p+A2)./(p+A3))+e.*log((-  
e+A4)./(-e+A5))+q.*log((-q+A6)./(-q+A7))+A1-A2-A7-  
A4+A3-Z+A6-A5);  
M3=(mu.*Np.*Ns)./(4.*pi).*(B1-B2+B3-B4);  
eff2=(RL./(RL+Rs)).*(1./(1+Rp.*(RL+Rs)./(w.^2.*M3.^2)))*  
100;  
RL = 0:1:10;  
Qp1= (Lp.*RL)./(w.*M2.^2);  
Qs=(w.*Ls)./(RL);
```

```
Kd=1./((1+log(Qp1./Qs)).*(1+log(fm./f)));  
title('Plot:RLvsKd plot');  
plot(RL,Kd)  
xlabel('load resistance ')  
ylabel('Distribution factor')  
legend('RLvsKd curve');  
grid;
```

### Plot for height vs. efficiency

```
h=0:0.1:0.5;  
A=sqrt(h.^2+t.^2+d.^2);  
B=sqrt(h.^2+d.^2+q.^2);  
C=sqrt(h.^2+q.^2+g.^2);  
D=sqrt(h.^2+g.^2+t.^2);  
E=sqrt(h.^2+q.^2+c.^2);  
F=sqrt(h.^2+c.^2+t.^2);  
G=sqrt(h.^2+t.^2+m.^2);  
H=sqrt(h.^2+m.^2+q.^2);  
B1=(d.*log((d+A)./(d+B))+h.*log((g+C)./(g+D))+c.*log((-  
c+E)./(-c+F))+m.*log((-m+G)./(-m+H))+B-C-H+E+D-A+G-  
F);  
I=sqrt(h.^2+p.^2+d.^2);  
J=sqrt(h.^2+d.^2+e.^2);  
K=sqrt(h.^2+e.^2+g.^2);  
L=sqrt(h.^2+p.^2+h.^2);  
M=sqrt(h.^2+e.^2+c.^2);  
N=sqrt(h.^2+c.^2+p.^2);  
O=sqrt(h.^2+p.^2+m.^2);  
P=sqrt(h.^2+m.^2+e.^2);  
Q=sqrt(h.^2+p.^2+g.^2);  
B2=(d.*log((d+h)./(d+J))+g.*log((h+K)./(g+L))+c.*log((-  
c+M)./(-c+N))+m.*log((-m+O)./(-m+P))+J-K-P+M+Q-I+O-  
N);  
R=sqrt(h.^2+g.^2+t.^2);  
S=sqrt(h.^2+t.^2+c.^2);  
T=sqrt(h.^2+p.^2+c.^2);  
U=sqrt(h.^2+g.^2+p.^2);  
V=sqrt(h.^2+e.^2+c.^2);  
W=sqrt(h.^2+e.^2+g.^2);  
X=sqrt(h.^2+g.^2+q.^2);  
Y=sqrt(h.^2+c.^2+q.^2);  
B3=(t.*log((t+R)./(t+S))+p.*log((p+T)./(p+U))+e.*log((-  
e+V)./(-e+W))+q.*log((-q+X)./(-q+Y))+S-T-Y+V+U-R+X-  
W);  
Z=sqrt(h.^2+d.^2+t.^2);  
A1=sqrt(h.^2+t.^2+m.^2);  
A2=sqrt(h.^2+m.^2+p.^2);  
A3=sqrt(h.^2+d.^2+p.^2);  
A4=sqrt(h.^2+e.^2+m.^2);  
A5=sqrt(h.^2+e.^2+d.^2);  
A6=sqrt(h.^2+d.^2+q.^2);  
A7=sqrt(h.^2+m.^2+q.^2);
```

```
B4=(t.*log((t+Z)./(t+A1))+p.*log((p+A2)./(p+A3))+e.*log((-e+A4)./(-e+A5))+q.*log((-q+A6)./(-q+A7))+A1-A2-A7-A4+A3-Z+A6-A5);
M3=(mu.*Np.*Ns)./(4.*pi).*(B1-B2+B3-B4);
eff2=(RL./(RL+Rs)).*(1./(1+Rp.*(RL+Rs)./(w.^2.*M3.^2)))*100;
title('The plot: Height vs. Efficiency');
plot(h,eff2);
xlabel('height in meters')
ylabel('Efficiency')
legend('height-efficiency curve');
grid;
```

#### Plot of Load vs. Efficiency

```
RL=1:1:10;
A=sqrt(h.^2+t.^2+d.^2);
B=sqrt(h.^2+d.^2+q.^2);
C=sqrt(h.^2+q.^2+g.^2);
D=sqrt(h.^2+g.^2+t.^2);
E=sqrt(h.^2+q.^2+c.^2);
F=sqrt(h.^2+c.^2+t.^2);
G=sqrt(h.^2+t.^2+m.^2);
H=sqrt(h.^2+m.^2+q.^2);
B1=(d.*log((d+A)./(d+B))+h.*log((g+C)./(g+D))+c.*log((-c+E)./(-c+F))+m.*log((-m+G)./(-m+H))+B-C-H+E+D-A+G-F);
I=sqrt(h.^2+p.^2+d.^2);
J=sqrt(h.^2+d.^2+e.^2);
K=sqrt(h.^2+e.^2+g.^2);
L=sqrt(h.^2+p.^2+h.^2);
M=sqrt(h.^2+e.^2+c.^2);
N=sqrt(h.^2+c.^2+p.^2);
O=sqrt(h.^2+p.^2+m.^2);
P=sqrt(h.^2+m.^2+e.^2);
Q=sqrt(h.^2+p.^2+g.^2);
B2=(d.*log((d+h)./(d+J))+g.*log((h+K)./(g+L))+c.*log((-c+M)./(-c+N))+m.*log((-m+O)./(-m+P))+J-K-P+M+Q-I+O-N);
R=sqrt(h.^2+g.^2+t.^2);
S=sqrt(h.^2+t.^2+c.^2);
T=sqrt(h.^2+p.^2+c.^2);
U=sqrt(h.^2+g.^2+p.^2);
V=sqrt(h.^2+e.^2+c.^2);
W=sqrt(h.^2+e.^2+g.^2);
X=sqrt(h.^2+g.^2+q.^2);
Y=sqrt(h.^2+c.^2+q.^2);
B3=(t.*log((t+R)./(t+S))+p.*log((p+T)./(p+U))+e.*log((-e+V)./(-e+W))+q.*log((-q+X)./(-q+Y))+S-T-Y+V+U-R+X-W);
Z=sqrt(h.^2+d.^2+t.^2);
A1=sqrt(h.^2+t.^2+m.^2);
A2=sqrt(h.^2+m.^2+p.^2);
A3=sqrt(h.^2+d.^2+p.^2);
A4=sqrt(h.^2+e.^2+m.^2);
```

```
A5=sqrt(h.^2+e.^2+d.^2);
A6=sqrt(h.^2+d.^2+q.^2);
A7=sqrt(h.^2+m.^2+q.^2);
B4=(t.*log((t+Z)./(t+A1))+p.*log((p+A2)./(p+A3))+e.*log((-e+A4)./(-e+A5))+q.*log((-q+A6)./(-q+A7))+A1-A2-A7-A4+A3-Z+A6-A5);
M3=(mu.*Np.*Ns)./(4.*pi).*(B1-B2+B3-B4);
eff2=(RL./(RL+Rs)).*(1./(1+Rp.*(RL+Rs)./(w.^2.*M3.^2)))*100;
title('The plot: Load vs. Efficiency');
plot(RL,eff2);
xlabel('load resistance in ohms')
ylabel('Efficiency')
legend('load-efficiency curve');
grid;
```

#### MATLAB input and Output

```
height in m =0.2
width of primary winding in m =0.6
width of secondary winding in m =0.6
length of primary winding in m =1
length of secondary winding in m =0.6
primary voltage in volts =150
load resistance in ohms =1.215
primary turns =6
secondary turns =6
primary surface area in mm^2 =38*10^(-6)
secondary surface area in mm^2 =28*10^(-6)
Resistivity of copper =1.72*10^(-8)
frequency in Hz=17702
Cp = 8.8617e-007
Cs = 1.2046e-006
Kd = 1.4050
Zs =1.2238 + 0.0000i
Zr1 = 2.3636 - 0.0000i
Zr2 = 1.5265 - 0.0000i
Zp1 = 2.3723 - 0.0000i
Zp2 = 1.5351 - 0.0000i
Ip1 = 63.2304 + 0.0000i
Ip2 = 97.7104 + 0.0000i
Is1 = 87.8716 - 0.0000i
Is2 = 1.0912e+002 -4.4832e-016i
V11 = 106.7640
V12 =132.5855
N-parameters are as follows
The number of primary turns np=6.000000
The number of secondary turns ns=6.000000
The primary surface area sp=0.000038
The secondary surface area ss=0.000028
The single side length of primary r1=0.008519
The single side length of secondary r2=0.007313
The primary winding resistance Rp=0.008691
The secondary winding resistance Rs=0.008846
The primary winding inductance Lp=0.000091
```



The secondary winding inductance  $L_s=0.000067$   
The mutual inductance without misalignment  $M_2=0.000015$   
The mutual inductance with misalignment  $M_3=0.000012$   
The coefficient of coupling without misalignment  $k_1=0.195450$   
The coefficient of coupling with misalignment  $k_2=0.157070$   
The frequency of the system  $f=17702.000000$   
The capacitance of the primary system  $C_1=0.000001$   
The capacitance of the secondary system  $C_2=0.000001$   
The secondary winding voltage without misalignment  $V_{11}=106.763968$   
The secondary winding voltage with misalignment  $V_{12}=132.585522$   
The quality factor of primary winding without misalignment  $Q_{p1}=4.261462$   
The quality factor of primary winding with misalignment  $Q_{p2}=6.598492$   
The quality factor of secondary winding  $Q_s=6.142859$   
The power transfer from primary to secondary without misalignment  $P_1=9449.819856$   
The power transfer from primary to secondary with misalignment  $P_2=14573.582478$   
The efficiency of the system without misalignment  $eff_1=0.989135$   
The efficiency of the system with misalignment  $eff_2=0.987152$

### MATLAB Plots

Fig 8 Load resistance vs. Distribution factor Plot

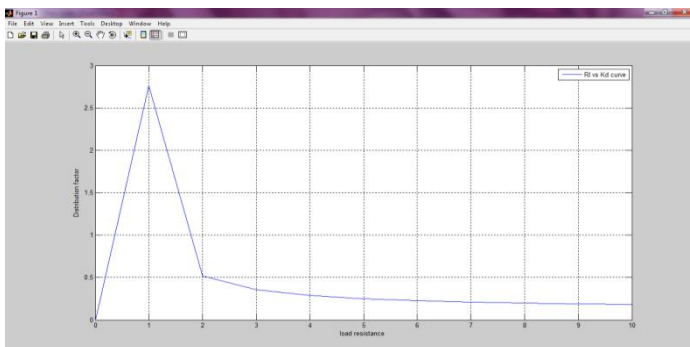


Fig 9 Height vs. Efficiency Plot

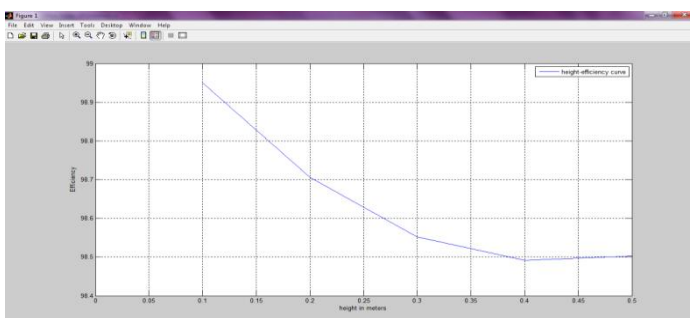
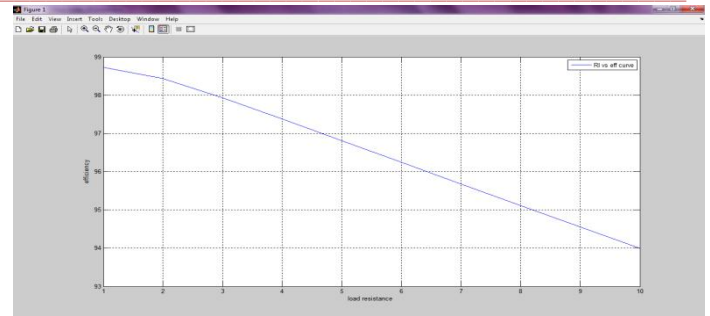


Fig 10 Load vs. Efficiency Plot



### IX.IMPLEMENTED CIRCUIT DIAGRAM

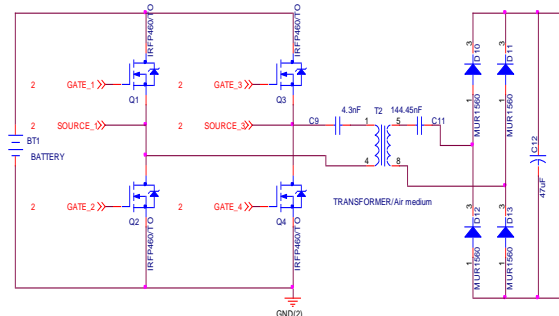


Fig 11 Circuit Diagram for WPT

### DESCRIPTION OF COMPONENTS

#### PWM Controller UCC3895

**UCC3895** is used as a phase shift PWM controller. It implements control of a full-bridge power stage by phase shifting the switching of one half-bridge with respect to the other. It allows constant frequency pulse-width modulation in conjunction with resonant zero-voltage switching to provide high efficiency at high frequencies. The part can be used either as a voltage-mode or current-mode controller.

Its additional features are - enhanced control logic, adaptive delay set, and shutdown capability. It operates with dramatically less supply current than its bipolar counterparts. The UCC3895 can operate with a maximum clock frequency of 1 MHz

Pin diagram of UCC3895 is given below:

#### PWM CONTROLLER

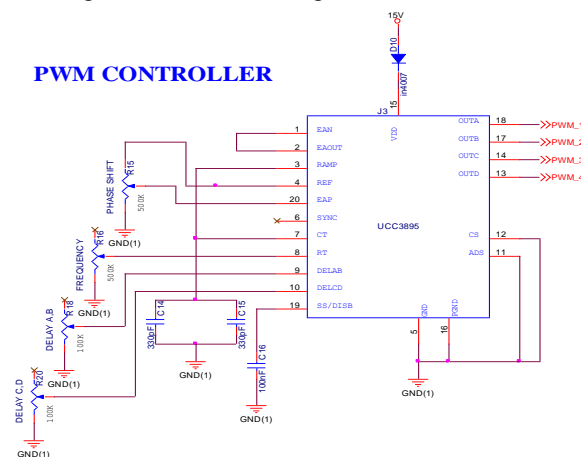
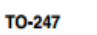


Fig 12 Pin Diagram of UCC3895

**POWER SUPPLY FOR THE CONTROLLER**

**MOSFET IRFP460**

**TO-247**



The image shows a TO-247 package, which is a three-terminal power semiconductor package. It is a black, rectangular component with three pins extending from one end. The pins are labeled S (Source), D (Drain), and G (Gate). To the right of the package is the schematic symbol for an N-Channel MOSFET. The symbol shows a vertical line for the Drain (D) at the top, a horizontal line for the Source (S) at the bottom, and a gate (G) on the left. The symbol also includes a small circle on the gate and a triangle on the drain, indicating the N-channel type.

N-Channel MOSFET

MOSFET IRFP460 and MOSFET symbol

- Dynamic dV/dt Rating
- Repetitive Avalanche Rated
- Isolated Central Mounting Hole
- Fast Switching
- Ease of Paralleling
- Simple Drive Requirements

## MOSFET Driver IR2101

- 1)  $V_{\text{OFFSET}}$  600V max.
- 2)  $IO_{+/-}$  130 mA / 270 mA
- 3)  $V_{\text{OUT}}$  10 - 20V
- 4)  $t_{\text{on/off}}$  (typ.) 160 & 150 ns
- 5) Delay Matching 50 ns

- 1) Floating channel designed for bootstrap operation
- 2) Fully operational to +600V
- 3) Tolerant to negative transient voltage
- 4) dV/dt immune

- 5) Gate drive supply range from 10 to 20V
- 6) Under voltage lockout
- 7) 3.3V, 5V, and 15V logic input compatible
- 8) Matched propagation delay for both channels
- 9) Outputs in phase with inputs (IR2101) or out of phase with inputs (IR2102)
- 10) Also available LEAD-FREE

### ***Buffer Circuit CD4050B***

The CD4050B devices is non-inverting hex buffer, and feature logic-level conversion using only one supply voltage (VCC). The input-signal high level (VIH) can exceed the VCC supply voltage when these devices are used for logic level conversions. These devices are intended for use as CMOS to DTL or TTL converters and can drive directly two DTL or TTL loads. (VCC = 5 V, VOL ≤ 0.4 V, and IOL ≥ 3.3 mA.)

- CD4050B Non-inverting
- High Sink Current for Driving 2 TTL Loads
- High-to-Low Level Logic Conversion
- 100% Tested for Quiescent Current at 20 V
- Maximum Input Current of 1  $\mu$ A at 18 V Over Full Package Temperature Range; 100 nA at 18 V and 25°C
- 5-V, 10-V, and 15-V Parametric Rating

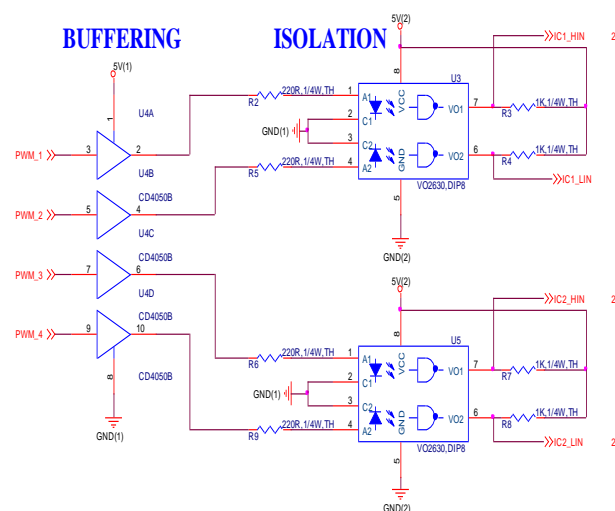


Fig 14 Buffer circuit with Optocoupler

## Switch-mode Power Rectifiers MUR1560

These state-of-the-art devices are a series designed for use in switching power supplies, inverters and as freewheeling diodes.

- Ultrafast 35 and 60 Nanosecond Recovery Time
- 175°C Operating Junction Temperature
- High Voltage Capability to 600 V
- ESD Ratings: ♦ Machine Model = C ♦ Human Body Model = 3B
- Low Forward Drop

- Low Leakage Specified @ 150°C Case Temperature
- Current De-rating Specified @ Both Case and Ambient Temperatures
- SUR8 Prefix for Automotive and Other Applications Requiring Unique Site and Control Change Requirements; AEC-Q101 Qualified and PPAP Capable
- All Packages are Pb-Free

#### Mechanical Characteristics:

- Case: Epoxy, Molded
- Weight: 1.9 Grams (Approximately)
- Finish: All External Surfaces Corrosion Resistant and Terminal Leads are Readily Solderable
- Lead Temperature for Soldering Purposes: 260°C Max. for 10 Seconds

#### Compensation Capacitors

The two series capacitors are used as compensation capacitors and are also used to get resonance condition. The values are:

Primary Capacitor = 4.3.nF

Secondary Capacitor = 144.45nF

## X. EXPERIMENTAL SETUP

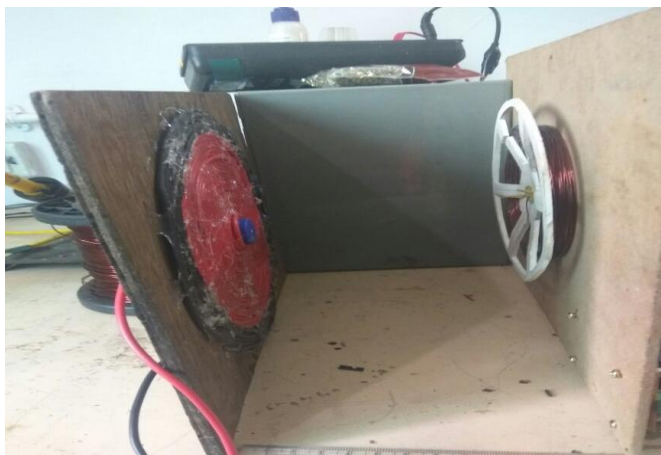


Fig 15 Primary and Secondary windings configuration

The figure shows the primary and secondary windings like a coreless transformer with air as the medium. The distance between the primary and secondary is maintained as 15cms and both are aligned properly.



Fig 16 Primary side driver circuit

The primary side converter with all the components fabricated is shown above. It consists of PWM controller, H-bridge inverter, MOSFET driver, buffer and optocoupler circuit along with the power supply. The input DC power is applied using 12V battery.

Waveforms generated at the input side are shown in the figure 9. The operating frequency is 100KHz

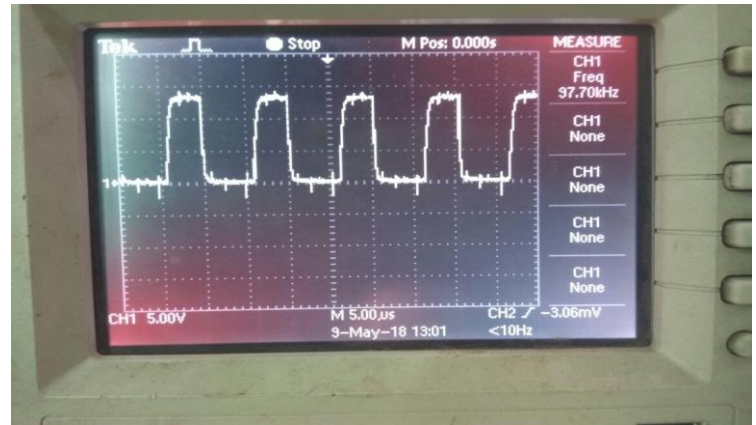


Fig 17 Waveform showing operating frequency 100KHz

TABLE I. EXPERIMENTAL RESULTS

SL. No.	Distance between the coils(cm)	Output Current (in mA)	Output Voltage(in V)
1.	5	2.5	10.4
2.	10	1.0	6.5
3.	15	0.5	4.1

## XI.CONCLUSION

This paper presents the simulated circuit and its input and output waveforms using the simulated model and the efficiency of the simulated circuit is seen for the different values of resistive load across the output side, it is observed as the efficiency of the system decreases as we increase the load. In this paper we implemented the hardware model for the wireless power transfer using the principle of inductive coupling and magnetic resonance. The various components used, their specifications and features along with the experimental setup is shown and evaluated. The readings were tabulated for different distances between primary and secondary windings. We were able to transfer power wirelessly for a distance of 15cms effectively which can be used for electric battery charging by modifying the circuit for higher power ratings.

## XII.FUTURE SCOPE

The charging of EV's using WPT system using is ICPT system is one of the promising technology, is growing due to depletion of the fuels, increasing and issues of global warming .But due to the decrease in efficiency of the hardware model and initial cost this technology of

charging the electric vehicles is not implemented Due to the fast moving technology further research is growing on to reduce the cost and efficiency therefore, This method of charging of EV'S can be implemented.

Recently research are going on for dynamic charging of electric vehicles i.e charging the electric vehicles while moving n the road. In future the same model can be implemented with higher power ratings for different application like electric vehicle charging. Stationary charging in future will give way to dynamic charging which is still under research

#### REFERENCE

- [1] [1]Villa JL, Llombart A, Sanz JF, Sall\_an J. Practical development of a 5 kW ICPT system SS compensated with a large air gap.IEEEIntSympInd Electron ISIE 2007;2007:1219e23.
- [2] [2] Ding P-P, Bernard L, Pichon L, Razek A. Evaluation of electromagnetic fields in human body exposed to wireless inductive charging system. IEEE Trans Magn 2014;50(2):1037e40.
- [3] [3] Chopra S. Contactless power transfer for electric vehicle charging application. Master of Science Thesis. Delft: Delft University of Technology, Faculty of Electrical Engineering, Mathematics and Computer Science Electrical Power Processing; 2011. p. 14e5.
- [4] [4] Gazulla JLV. Sistemas de Transferencia de Energia para VehiculosElectricosMedianteAcoplamientoInductivo.Doctoral Thesis. Zaragoza: Universidad de Zaragoza Departamento de IngenieriaElectrica; 2009. 2-7, 33-34, 45-55,68e69.
- [5] [5] Sall\_an J, Villa JL, Llombart A, Sanz JF. Optimal design of ICPT systems applied to electric vehicle battery charge. IEEE Trans Ind Electron 2009;56(6):2140e9.
- [6] [6] Ferdandez C, Garcia O, Prieto R, Cobos JA, Gabriels S, Borghet VD. Design issues of a core-less transformer for a Contact-less application. In: Applied Power Electronics Conference and Exposition, 2002. APEC 2002. Seventeenth Annual IEEE, vol. 1; 2002. p. 339e45.
- [7] [7] Hurley WG, Duffy MC. Calculation of self and mutual impedances in planar magnetic structures. IEEE Trans Magn 1995;31(4):2416e22.
- [8] [8] Wang C, Covic GA, Stielau OH. Power transfer capability and bifurcation phenomena of loosely coupled inductive power transfer systems. IEEE Trans Ind Electron 2004;51(1):148e57.
- [9] [9] Boeij J, Lomonova E, Vandenput A. Contactless energy transfer to a moving load Part I: topology synthesis and FEM simulation. IEEE IntSympInd Electron 2006;2:739e44.
- [10] [10] Bal G, Oncu S, Borekci S. Design and implementation of a self oscillating induction heater. J FacEng Arch GaziUniv 2011;26(4):771e6.
- [11] [11] Bal G, Oncu S, Ozbas E. Self-oscillated induction heater for absorption cooler. ElektronIrElektrotechnika 2013;19(10):45e8.
- [12] [12] Kim H, Song C, Kim D-H, Jung DH, Kim I-M, Kim II Y, et al. Coil design and measurements of automotive magnetic resonant wireless charging system for high-efficiency and low magnetic field leakage. IEEE Trans Microw Theory Tech2016;64(2):383e400.Zhang W, White JC, Malhan RK, Mi CC. Loosely coupled transformer coil design to minimize EMF radiation in concerned areas. IEEE Trans VehTechnol 2016;65(6):4779e89.
- [13] [17] Asa E, Colak K, Bojarski M, Czarkowski D. Asymmetrical duty-cycle and phase-shift control of a novel multiport CLL resonant converter. IEEE J EmergSel Top Power Electron 2015;3(4):1122e31.

#### AUTHORS

**JIGYASA CHAND** pursuing (8th-sem) B.E (Electrical & Electronics Engineering) in Dr. T. Thimmaiah Institute of Technology, K.G.F. VTU. Placed in TATA Consultancy Services (TCS). Area of Interest: Renewable Energy Sources, Network Analysis

**ANJALI.P.S** pursuing (8<sup>th</sup>-sem) B.E (Electrical & Electronics Engineering) in Dr. T. Thimmaiah Institute of Technology, K.G.F. VTU. Area of interest: Power System Planning and Renewable Energy Sources

**KIRTHIGA.G** (Electrical & Electronics Engineering) in Dr. T. Thimmaiah Institute of Technology, K.G.F. VTU *Eight Semester*)

**SOMASHEKAR. B** received B.E degree (Electrical & Electronics Engineering) from Golden Valley Institute of Technology, K.G.F in 1998, Bangalore University and M. Tech (VLSI & Embedded Systems) from BMS, VTU in 2010. He is currently working as an Assistant Professor in the Department of Electrical Engineering, Dr. TTIT, KGF. His research areas are Power Systems, wireless power systems, multiphase VLSI and Power Electronics.